Desalination and Water Treatment
www.deswater.com
doi: 10.5004/dwt.2023.29157

282 (2023) 139–145
January

Synthesis of functional hydrochar from pinewood wastes through hydrothermal carbonization for removal of Pb(II) ions from aqueous solutions

B.S. Naveen Prasad[a], Krishnan Saravanakumar[b], Sathiyamoorthy Manickkam[c], R. Senthilkumar[b], D.M. Reddy Prasad[d,*]

[a]*Department of Engineering, University of Technology and Applied Sciences, Salalah, Oman*
[b]*Department of Engineering, University of Technology and Applied Sciences, Suhar, Oman*
[c]*Department of Chemical Engineering, Higher Colleges of Technology, Ruwais Women's College, Abu Dhabi, United Arab Emirates*
[d]*Petroleum and Chemical Engineering Programme area, Faculty of Engineering, Universiti Teknologi Brunei, Brunei, email: dmr.Prasad@utb.edu.bn/dmrprasad@gmail.com*

Received 12 July 2022; Accepted 28 November 2022

ABSTRACT

Hydrothermal carbonization of pinewood wastes was performed to synthesize hydrochar for the removal of Pb(II) ions from contaminated solutions. The pinewood hydrochar was characterized using Fourier transform infrared, scanning electron microscopy, and X-ray diffraction. The results confirmed the porous nature of the hydrochar surface and the presence of various functional sites. The maximum Pb(II) uptake was recorded as 46.7 mg/g at pH 4.5. The experimental isotherm data exhibited a good fit to the Redlich–Peterson model, followed by the Langmuir and Freundlich models. The pseudo-first kinetics equation showed a better fit to Pb(II) kinetics data. Elution of Pb(II) ions from Pb(II)-loaded hydrochar was attempted using several elutants and the results indicated that 0.01 M HNO_3 performed well with elution efficiency over 99.7%. Regeneration tests were aimed to regenerate and reuse pinewood hydrochar for five cycles and the hydrochar performed well in all cycles with only a 4.9% decrease in adsorption capacity at the end of the fifth cycle.

Keywords: Adsorption; Hydrothermal carbonization; Hydrochar; Sustainability; Waste utilization

1. Introduction

Hydrothermal carbonization (HTC) is recently gaining a lot of attention worldwide as an effective and practical technique to convert waste biomasses to energy-dense, carbon-rich, and value-added solid hydrochars [1,2]. For several decades, adsorption using activated carbons was considered to be a practical technique for heavy metals removal from polluted streams [3,4]. However, activated carbons are costly to produce, and thus several research studies are focussing on identifying new viable adsorbents. Recently, biochar, a char-type material synthesized through the pyrolysis of biomaterials under an oxygen-free environment, has been validated as a valuable adsorbent for heavy metals [5–7]. Biochar can be produced via several modes and the most popular mode of heat treatment (pyrolysis) presents several limitations such as low solid (biochar) yield and being expensive [1]. Owing to this, an alternate way to produce char, including hydrothermal carbonization is gaining momentum [8].

HTC is a thermo-chemical process, wherein biomaterials are exposed to sub-critical water to form a solid residue termed hydrochar. Hydrochar is basically rich in carbon comprising acidic binding sites. They are less aromatic

* Corresponding author.

compared to biochar materials and are mostly comprised of alkyl moieties [9]. HTC has several advantages over other pyrolytic techniques, including low-temperature requirement (180°C–350°C) under autogenous pressure in the presence of water as well as non-requirement of the drying process for wet feedstock. In addition, hydrochar retains a maximum portion of C from the feedstock thereby reducing greenhouse emissions [10]. Hydrochar found applications in various fields, including solid fuels, soil amendments, nutrient recovery, carbon sequestration, and adsorption [11]. In recent years, hydrochar is garnering significant attention as an adsorbent for several pollutants, including organics, nutrients, and heavy metal ions [2,12–14]. Hydrochar performed well in the binding of pollutants on account of excessive acidic binding sites. Dhaouadi et al. [15] prepared hydrochars from avocado seed and utilized them for heavy metals sorption. The authors accounted that hydrochar comprises approximately 37% of total acidic functional groups. This facilitates superior heavy metal adsorption with uptake capacities in the range of 0.12–0.35 mmol/g. Nevertheless, research studies performed to understand the adsorption potential of hydrochar were less compared to biochar. More studies are needed to understand the adsorption properties as well as mechanisms associated with hydrochar performance.

Thus, the present study aimed to prepare hydrochar from pinewood waste for the adsorption of Pb(II) ions from contaminated solutions. Several kinetic and isotherm models were utilized to characterize the experimental data as well regeneration studies were aimed to understand the reusability of hydrochar for multiple sorption–elution cycles.

2. Materials and methods

2.1. Feedstock, hydrochar, and adsorbate preparation

Pinewood mulch was purchased from a local nursery (Oman). It was then cleaned extensively with distilled water and subsequently dried for 6 h at 105°C. The dried mulch was crushed to obtain particles of 0.75 mm (average size diameter). The stock Pb(II) solution was prepared using analytical grade lead nitrate salt (Sigma-Aldrich)

Hydrothermal carbonization was performed using a 0.5 L Parr autoclave semi-batch reactor (USA). About 10 g of grounded pinewood mulch was contacted with 150 mL distilled water inside the reactor and the autoclave was heated to 300°C. The reactor was maintained at 300°C for 1 h and subsequently cooled quickly to room temperature. The solid residue (hydrochar) was recovered from the slurry through vacuum filtration and dried in an oven for 24 h at 105°C.

2.2. Hydrochar characterization

Scanning Electron Microscope (Hitachi-S4800, Japan) was utilized to analyze the hydrochar surface. The samples were spread on a copper grid before photographs were taken. Fourier-transform infrared (FTIR) spectra of samples were taken using the KBr pellet procedure between 400 and 4,000 cm^{-1} in Bruker-ATR IR (Germany). X-ray diffraction (XRD) analyses of samples were carried out in Bruker D8 Advance (Germany) to identify the crystallographic structure.

2.3. Experimental procedure

The experiments were aimed to study the effects of initial Pb(II) concentrations, equilibrium pH, and contact times on the removal of the Pb(II) ions from solutions. For adsorption experiments, 0.1 g of hydrochar (adsorbent) was contacted with 100 mL of Pb(II) (adsorbate) solution of known concentration (10–100 mg/L) in a 250 mL flask. The pH of this mixture was initially adjusted and controlled throughout the experiments using 0.1 M NaOH/HCl. The mixture was then agitated in a shaker at 160 rpm for 6 h. After 6 h, the mixture was filtered using a syringe filter (0.45 μm poly(tetrafluoroethylene)) to separate the hydrochar from the mixture. The filtrate was then analyzed for Pb(II) concentrations in an Inductively Coupled Plasma-Optical Emission Spectrometer (ICP-OES) (Perkin Elmer Optima 5300 DV). The desorption experiments were conducted by contacting metal-loaded hydrochar separately with distilled water, acidic (0.01 M nitric acid, 0.01 M hydrochloric acid, and 0.01 M sulfuric acid), and alkaline (0.01 M sodium hydroxide) elutants. The reaction time was fixed at 60 min and the remaining experimental methods were the same as that of adsorption trials.

2.4. Data modelling

To fit the data derived from experiments, selected kinetic and isotherm models were utilized, including,

Langmuir model: $$Q = \frac{Q_{\max} \cdot C_f \cdot b_L}{1 + C_f \cdot b_L} \quad (1)$$

Freundlich model: $$Q = K_F \cdot C_f^{1/nF} \quad (2)$$

Redlich–Peterson model: $$Q = \frac{K_{RP} C_f}{1 + a_{RP} C_f^{\beta_{RP}}} \quad (3)$$

where Q is the sorption capacity of hydrochar towards Pb(II) ions (mg/g); C_f is the equilibrium concentration of Pb(II) ions in solution (mg/L); $Q_{\max}$ is the maximum Pb(II) uptake of hydrochar (mg/g); b_L is the Langmuir model equilibrium constant (L/mg); K_F is the Freundlich model constant (mg/g) $(L/mg)^{1/nF}$; n_F is the Freundlich model exponent; a_{RP} is the Redlich–Peterson constant (L/mg), β_{RP} is the Redlich–Peterson exponent, and K_{RP} is the Redlich–Peterson constant (L/g).

The kinetics models employed to evaluate Pb(II) adsorption data includes,

Pseudo-first-order model: $$Q_t = Q_e\left(1 - \exp\left(-k_1 t\right)\right) \quad (4)$$

Pseudo-second-order model: $$Q_t = \frac{Q_e^2 k_2 t}{1 + Q_e k_2 t} \quad (5)$$

where Q_e is the equilibrium sorption uptake of hydrochar towards Pb(II) ions (mg/g), k_1 and k_2 are the pseudo-first-order and pseudo-second-order model constants, respectively, and Q_t is the sorption uptake at time t (mg/g).

The percentage error was calculated using the following equation,

$$\varepsilon(\%) = \frac{\sum_{i=1}^{N}\left(Q_{\exp,i} - Q_{\text{calc},i} / Q_{\exp,i}\right)}{N} \times 100 \quad (6)$$

where N is the number of trials; $Q_{\exp}$ (mg/g) and Q_{calc} (mg/g) refers to the experimental uptake value and model-calculated uptake value, respectively.

All model equations were solved using Sigma Plot software (USA) through non-linear regression. All trials were performed twice and error bars were provided for all experimental data.

3. Results and discussion

3.1. Instrumental analysis

The FTIR analyses of feedstock and hydrochar samples are presented in Fig. 1. Generally, considerable differences in the presence/extent of binding sites were perceived in pinewood and hydrochar samples. Specifically, the broad band (3,600–3,100 cm^{-1}) which represents the O–H stretching subsided with the formation of hydrochar, owing to dehydration of feedstock. The C–H stretching (symmetric and asymmetric) (2,800–2,900 cm^{-1}) was less intense and almost disappeared in the hydrochar sample. The peak at 1,600 cm^{-1} related to C=C stretching (possibly aromatic ring in cellulose) in feedstock, the declined in intensity with the formation of hydrochar due to the disintegration of high molecular weight compounds. In feedstock, an intense band was observed at nearly 1,000 cm^{-1} and this can be assigned to stretching of C–O bonds (e.g., carboxyl, ethanol, phenol, and hydroxyl, etc.), and/or $–OCH_3$ (aliphatic groups) [16], and the peak intensity remarkably declined in hydrochar. Overall, the characterization of feedstock and hydrochar using the above-mentioned multiple techniques indicates that hydrothermal carbonization had a positive influence on the augmentation of various surface properties including surface area and carbon contents. Thus, it is expected that the synthesized hydrochar could be considered a cost-efficient sorbent for the removal of metal ions from solutions.

Fig. 2 shows the XRD of pinewood and hydrochar. At 2θ values of 15° and 22°, two broad peaks were detected for the pinewood sample. These peaks can be related to 1 0 1 and 0 0 2 lattice spacings of cellulose in pinewood [7]. In the case of hydrochar, these peaks disappeared owing to the damage of cellulose. This vanishes the crystallinity of the hydrochar sample, taking into consideration that hemicellulose and lignin are essentially amorphous [17]. Hence, the synthesized hydrochar showed the typical character of an amorphous material.

Fig. 3 presents scanning electron analyses of pinewood and hydrochar. As expected, both samples showed a distinctive structure with unique pore sizes and shapes. In the case of pinewood, the surface was observed to be fibrous without the major presence of pores. With hydrothermal carbonization, new pores were created on the surface of the hydrochar. The hydrochar surface also became uneven owing to increased carbonisation/aromatisation. Honeycomb like structure was detected in the hydrochar sample, which supports the potential adsorption capacity of produced hydrochar.

3.2. Influence of pH

The equilibrium pH is a very important physicochemical parameter that impacts the solution chemistry of metal ions and surface properties of char material [18]. In an attempt to assess the importance of pH, the equilibrium pH of hydrochar-Pb(II) suspension was changed from 2 to 5 (Fig. 4). The experimental outcome indicated that equilibrium pH strongly influenced the interaction of Pb(II) ions toward hydrochar (Fig. 4). In general, the sorption of Pb(II) ions enhanced with a surge in equilibrium pH with the highest uptake achieved at pH 4.5. This surge in uptake as the equilibrium pH shift from strongly acidic to mildly acidic is due to multiple reasons. Specifically, Pb exists as

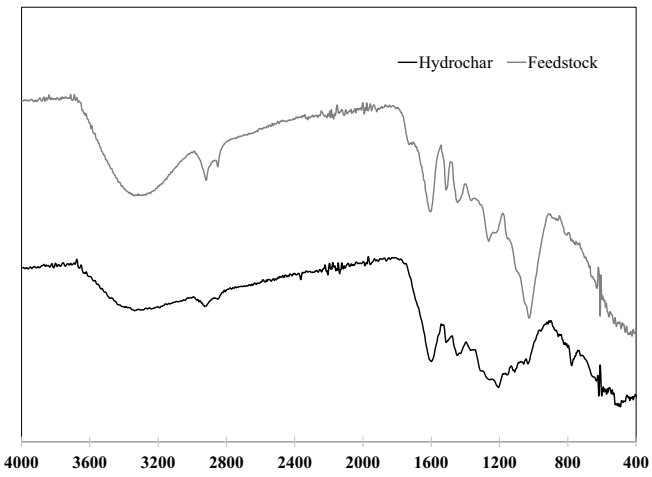

Fig. 1. FTIR spectra of feedstock and hydrochar.

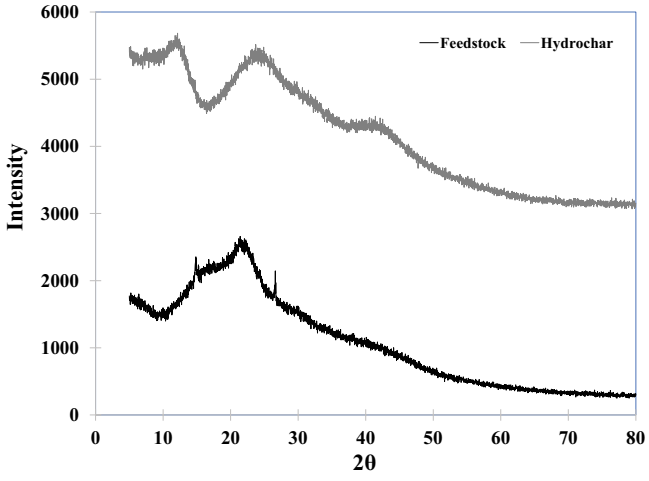

Fig. 2. XRD patterns of feedstock and hydrochar.

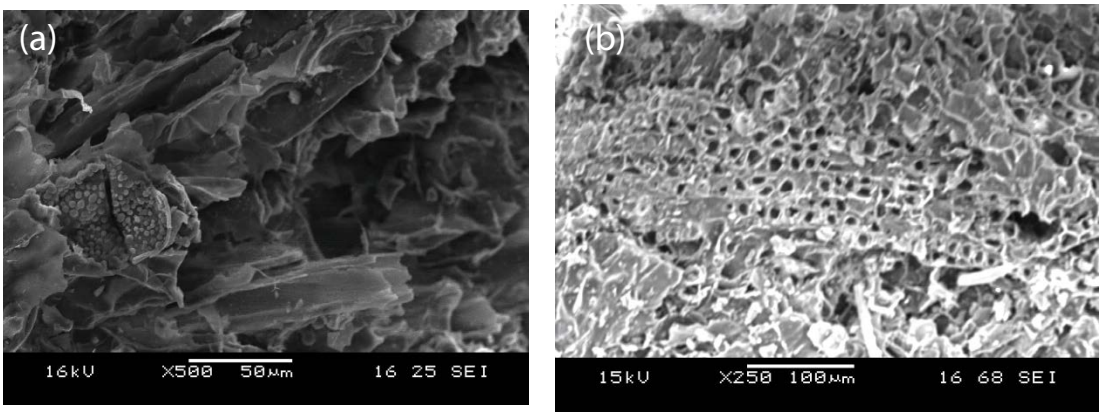

Fig. 3. SEM photographs of (a) feedstock and (b) hydrochar.

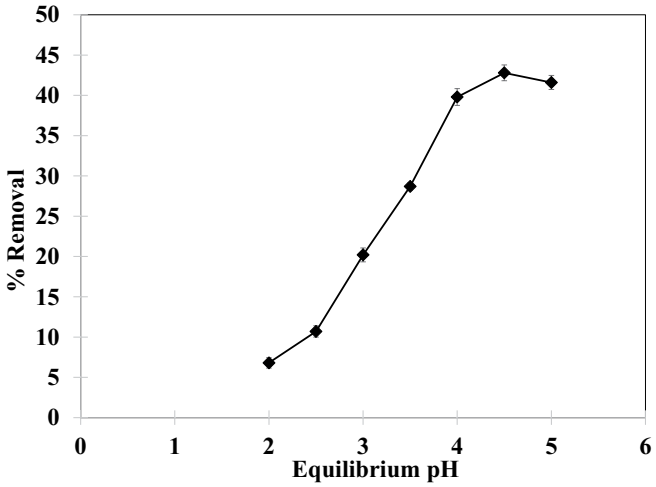

Fig. 4. Influence of equilibrium pH on Pb(II) removal by hydrochar (initial Pb(II) concentration = 100 mg/L; temperature = 30°C ± 1°C).

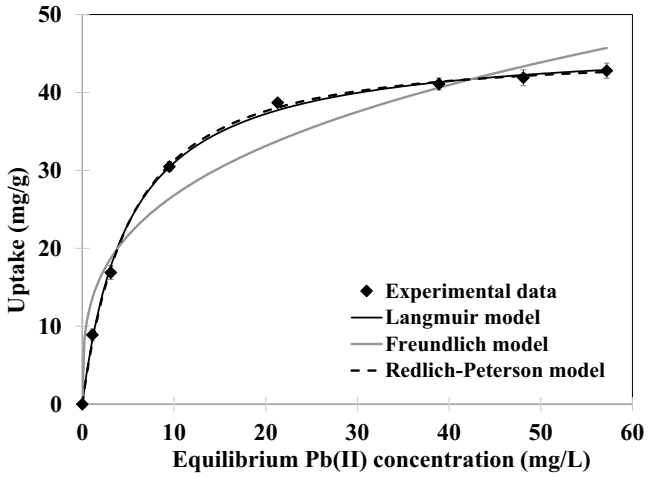

Fig. 5. Equilibrium Pb(II) isotherm and model prediction (pH = 4.5; temperature = 30°C ± 1°C).

Pb(II) (divalent form) in solutions under pH 5.0 [19,20]. In strongly acidic solutions, excess H^+ ions occupy binding sites of hydrochar rather than the divalent metal ion of interest thereby causing protonation of the hydrochar surface [21]. This results in less Pb(II) uptake by hydrochar. As the pH increases (strong acidic to mild acidic), the abundance of H^+ ions decreases which enables more Pb(II) ions to occupy hydrochar binding sites, and subsequently improves Pb(II) uptake. In the current study, The Pb(II) uptake of 6.8 mg/g achieved at pH 2 surged to 42.8 mg/g at pH 4.5.

3.3. Isotherm and modeling

Adsorption isotherm is critical to evaluate the maximum sorption potential of an adsorbent and the affinity of metal ions towards sorbent [22,23]. For this experiment, the initial Pb(II) concentration was changed from 10–100 mg/L at pH 4.5 (Fig. 5). The results specified that a favorable isotherm with a sharp slope was obtained for Pb(II) sorption onto hydrochar. The concave-shaped isotherm with a sharp slope confirms that hydrochar showed high affinity towards Pb(II) ions [24]. The adsorption potential of hydrochar enhanced with a surge in initial Pb(II) concentrations and reached a plateau at 100 mg Pb(II)/L with highest Pb(II) uptake of 42.8 mg/g.

Several isotherm models were employed to evaluate the nature of sorption and the mechanism of removal. The models employed include the Langmuir, Freundlich, and Redlich–Peterson models. Table 1 illustrates the isotherm model constants and error values. The two-parameter Langmuir model is a well-established equation to describe adsorption isotherm, which involves two-parameters Q_{max} and b_L [25]. The constant Q_{max} refers to the maximum uptake achievable even beyond experimental conditions. The constant b_L refers to extent of affinity between the solute and sorbent. For the Pb-hydrochar system, the Q_{max} and b_L values were 46.7 mg/g and 0.197 L/mg, respectively. Also, the Langmuir model predicted the experimental data reliably with low error and high R^2 (correlation coefficient) values (Table 1). Table 2 compares Pb(II) adsorption capacity of different sorbents reported in the literature.

The Freundlich equation is principally empirical in nature; nevertheless, it was also utilized to evaluate

Table 1
Isotherm model parameters during adsorption of Pb(II) ions by hydrochar

Langmuir	Q_{max} (mg/g)	46.7
	b_L (L/mg)	0.197
	R^2	0.997
	% error	0.28
Freundlich	K_F (mg/g) $(L/mg)^{1/nF}$	13.2
	n_F	3.27
	R^2	0.961
	% error	1.89
Redlich–Peterson	K_{RP} (L/g)	8.59
	a_{RP} $(L/mg)^{1/\beta RP}$	0.163
	β_{RP}	1.03
	R^2	0.999
	% error	0.14

Table 2
Comparison of Pb(II) uptake capacity by different adsorbents

Adsorbent	Uptake capacity (mg/g)	References
Activated carbon (waste rubber tires)	9.68	[31]
Biochar (from chicken feather)	40.9	[32]
Cocoa pod husk	20.1	[33]
Coal fly ash	45.6	[34]
Fungus (*Cephalosporium aphidicola*)	36.9	[35]
Oil palm frond	5.32	[36]
Hydrochar	46.7	This study

heterogeneous surfaces with binding groups of different affinities [26]. The model is assumed that the stronger functional groups are occupied first and that the binding strength declines as the degree of occupied sites surges. The constant which refers to the binding strength of the adsorbent, K_F, was recorded as 13.2 $(mg/g)(L/mg)^{1/nF}$; while the constant which indicates the affinity between hydrochar and Pb(II) ions was observed as 3.27. It should be noted that the fitting of data by the Freundlich model was not reasonable as observed in Fig. 5, supported by comparatively high % error and low R^2 values (Table 1). It can also be seen from Fig. 5 that the model-predicted curve was unable to reach a plateau as equilibrium concentration surges. The Redlich–Peterson equation is a three-parameter model, which integrates the attributes of Langmuir and Henry's model [27]. Due to the additional parameter, the Redlich–Peterson model performed well in the prediction of Pb(II) adsorption by hydrochar as evidenced by low error and high R^2 values (Table 1). As depicted in Table 1, the β_{RP} value was close to the unity, supporting that the Pb(II) adsorption by hydrochar was more of Langmuir's model. The isotherm data estimated by all model equations are illustrated in Fig. 5.

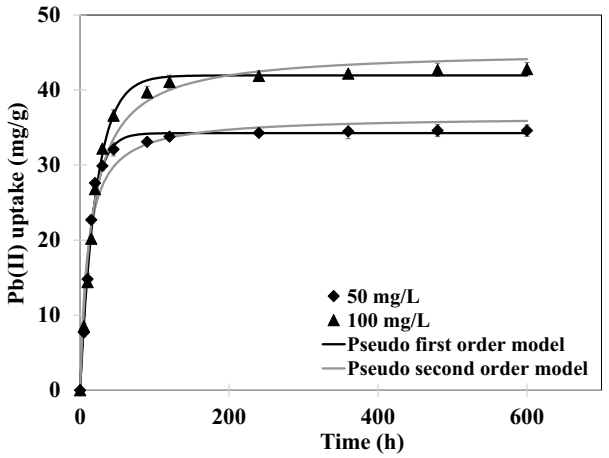

Fig. 6. Pb(II) kinetics and model prediction (pH = 4.5; temperature = 30°C ± 1°C).

3.4. Kinetic and modeling

Shown in Fig. 6 are the plots of Pb(II) uptake against time (sorption kinetics) for hydrochar at different initial Pb(II) concentrations. The evaluation and proper understanding of sorption kinetics are crucial to designing wastewater treatment schemes, as it provides crucial information into the adsorption mechanisms and reaction pathways as well as the determination of residence time [28]. In the case of the lowest Pb(II) concentration (50 mg/L), the metal uptake rate was very fast, with almost 90% total metal ion removal occurred within 45 min. At the end of this fast adsorption phase, the rate of metal uptake decreased and the final equilibrium was achieved in 240 min. These dual phases are commonly observed in most adsorption systems owing to the presence of large exchangeable binding groups on the surface of the adsorbent at the start of the process. As the adsorption proceeds, these binding groups got saturated and eventually, the rate declines and the system reached equilibrium [29]. Among the different initial Pb(II) concentrations examined (50–100 mg/L), the rate of sorption decreased at higher initial Pb(II) concentration as evidenced in Fig. 6; however, the equilibrium was found to be rapid and achieved within 240 min. It is also worth noting that the Pb(II) sorption capacity surged whereas the total % removal declined on increasing the initial Pb(II) concentrations. For example, the Pb(II) sorption capacity increased from 34.6 to 42.8 mg/g on increasing the initial Pb(II) concentrations from 50 to 100 mg/L. However, the % Pb(II) removal declined from 69.2% to 42.8% when Pb(II) concentrations increased from 50 to 100 mg/L. The reason for this behavior is due to the fact that the ratio of the initial moles of Pb(II) ions to the available surface area was low at lower concentrations, and thus the fractional adsorption was not dependent on initial concentrations [22]. Nevertheless, the functional binding groups on the adsorbent surface become less compared to the moles of Pb(II) ions present at higher Pb(II) concentrations, and thus the % Pb(II) removal was dependent on the initial Pb(II) concentrations.

The pseudo-first-order and pseudo-second-order kinetic equations were utilized to evaluate the experimental Pb(II)

Table 3
Kinetic model parameters during adsorption of Pb(II) ions by hydrochar

Model		Pb(II)	
		50 mg/L	100 mg/L
Uptake estimated experimentally (mg/g)		34.6	42.8
Pseudo-first-order	k_1 (min^{-1})	0.067	0.046
	Q_e (mg/g)	34.3	42.0
	R^2	0.989	0.997
	% error	0.49	0.27
Pseudo-second-order	k_2 (g/(mg·min))	0.0027	0.0014
	Q_e (mg/g)	36.5	45.3
	R^2	0.963	0.983
	% error	2.47	1.74

kinetic data. Table 3 presents the model-predicted Pb(II) uptake capacities, rate constants, % error, and R^2 values. The pseudo-first-order model provided a good fit to the Pb(II) kinetics with low % error (0.27%–0.49%) and high R^2 (0.989–0.997) values. The model was also able to predict the equilibrium sorption uptake with good accuracy. The rate constant (k_1) decreased, whereas uptake capacity surged as the initial Pb(II) concentration increased. Similarly, the pseudo-second-order equation provided low % error and high R^2 values for Pb(II) adsorption kinetics (Table 3). Nevertheless, the model unable to predict the experimental sorption uptake. The kinetic data as estimated by the pseudo-first-order and pseudo-second-order models for adsorption of Pb(II) ions by hydrochar are shown in Fig. 6.

3.5. Elution

Regeneration and reuse of sorbent material is crucial for the commercial success of the overall adsorption process. For this, the proper selection of elutant which necessitates repeated usage of sorbent without inflicting structural damage to the adsorbent is important [30]. To identify a practical and effective elutant for Pb(II)-loaded hydrochar, several eluants were examined, including 0.01 M HCl, HNO_3, H_2SO_4, NaOH, and distilled water. All acidic eluants performed well in the desorption of Pb ions from hydrochar with elution efficiencies of 99.5%, 99.7%, and 98.4%, recorded for 0.01 M HCl, HNO_3, and H_2SO_4, respectively. These results are in direct correlation with the effect of pH trails as shown in Fig. 4, which clearly indicates that low pH values provided very low adsorption percentages as a result of the protonation of hydrochar. On the other hand, control experiments conducted using distilled water indicated that Pb ions exhibited a very strong affinity towards hydrochar as a very low elution efficiency of 1.7% was obtained. Similarly, elution was also not favorable in alkaline environments as 0.01 M NaOH provided only 3.1% elution efficiency.

3.6. Regeneration

Additional experiments were conducted to examine the regeneration of hydrochar in repeated adsorption–elution cycles. The Pb(II) uptake capacities of hydrochar in five consecutive cycles were in the range of 40.7–42.8 mg/g. The elution efficiency exhibited by 0.01 M HNO_3 in all five cycles was greater than 99.6%. After five cycles of sorption/desorption, the hydrochar weight loss was less than 3.5%.

4. Conclusions

The present research established the feasibility of utilizing pinewood-derived hydrochar for the removal of Pb(II) ions from contaminated solutions. Characterization studies using FTIR, scanning electron microscopy (SEM), and XRD indicated that hydrothermal carbonization had positive influence on augmentation of various surface properties including surface area and carbon contents. The equilibrium pH studies confirmed that solution pH greater than 4 was required to obtain optimum Pb(II) adsorption. Adsorption isotherm obtained at pH 4.5 was described using the Langmuir, Freundlich and Redlich–Peterson models. At pH 4.5, the hydrochar produced a maximum Pb(II) uptake capacity of 46.7 mg/g, according to the Langmuir model. Adsorption kinetic experiments indicated that the rate of Pb(II) uptake was very fast, with equilibrium being attained within 4 h. The pseudo-first-order kinetic model was found to predict the Pb(II) kinetics data with high R^2 and low % error. Elution of Pb(II) ions from the Pb(II)-loaded hydrochar was successful using 0.01 M HNO_3. The hydrochar regeneration experiment was conducted for five cycles, without significant loss in the adsorption capacity of hydrochar. Thus, the current study identified a cost-effective, and efficient adsorbent for removal of Pb(II) ions from wastewaters. Additional research is required to evaluate the effectiveness of hydrochar in column mode.

Data availability statement

The data that support the findings of this study are available from the corresponding author, [DMRP], upon reasonable request.

References

[1] H.S. Kambo, A. Dutta, A comparative review of biochar and hydrochar in terms of production, physico-chemical properties and applications, Renewable Sustainable Energy Rev., 45 (2015) 359–378.
[2] Z. Liu, Z. Wang, H. Chen, T. Cai, Z. Liu, Hydrochar and pyrochar for sorption of pollutants in wastewater and exhaust gas: a critical review, Environ. Pollut., 268 (2021) 115910, doi: 10.1016/j.envpol.2020.115910.
[3] A. Bhatnagar, M. Ji, Y.-H. Choi, W. Jung, S.-H. Lee, S.-J. Kim, G. Lee, H. Suk, H.-S. Kim, B. Min, S.-H. Kim, B.-H. Jeon, J.-W. Kang, Removal of nitrate from water by adsorption onto zinc chloride treated activated carbon, Sep. Sci. Technol., 43 (2008) 886–907.
[4] C. Sukumar, V. Janaki, K. Vijayaraghavan, S. KamalaKannan, K. Shanthi, Removal of Cr(VI) using co-immobilized activated carbon and *Bacillus subtilis*: fixed-bed column study, Clean Technol. Environ. Policy, 19 (2017) 251–258.
[5] B. Qiu, X. Tao, H. Wang, W. Li, X. Ding, H. Chu, Biochar as a low-cost adsorbent for aqueous heavy metal removal: a review, J. Anal. Appl. Pyrolysis, 155 (2021) 105081, doi: 10.1016/j.jaap.2021.105081.
[6] B.K. Biswal, K. Vijayaraghavan, D.L. Tsen-Tieng, R. Balasubramanian, Biochar-based bioretention systems for removal

of chemical and microbial pollutants from stormwater: a critical review, J. Hazard. Mater., 422 (2022) 126886, doi: 10.1016/j.jhazmat.2021.126886.
[7] K. Vijayaraghavan, R. Balasubramanian, Application of pinewood waste-derived biochar for the removal of nitrate and phosphate from single and binary solutions, Chemosphere, 278 (2021) 130361, doi: 10.1016/j.chemosphere.2021.130361.
[8] A.A. Azzaz, B. Khiari, S. Jellali, C.M. Ghimbeu, M. Jeguirim, Hydrochars production, characterization and application for wastewater treatment: a review, Renewable Sustainable Energy Rev., 127 (2020) 109882, doi: 10.1016/j.rser.2020.109882.
[9] E. Taskin, C.C. Bueno, I. Allegretta, R. Terzano, A.H. Rosa, E. Loffredo, Multianalytical characterization of biochar and hydrochar produced from waste biomasses for environmental and agricultural applications, Chemosphere, 233 (2019) 422–430.
[10] G.K. Parshetti, H.S. Kent, R. Balasubramanian, Chemical, structural and combustion characteristics of carbonaceous products obtained by hydrothermal carbonization of palm empty fruit bunches, Bioresour. Technol., 135 (2013) 683–689.
[11] Z. Zhang, Z. Zhu, B. Shen, L. Liu, Insights into biochar and hydrochar production and applications: a review, Energy, 171 (2019) 581–598.
[12] L. Wu, W. Wei, D. Wang, B.-J. Ni, Improving nutrients removal and energy recovery from wastes using hydrochar, Sci. Total Environ., 783 (2021) 146980, doi: 10.1016/j.scitotenv.2021.146980.
[13] J. Wang, Y. Wang, J. Wang, G. Du, K.Y. Khan, Y. Song, X. Cui, Z. Cheng, B. Yan, G. Chen, Comparison of cadmium adsorption by hydrochar and pyrochar derived from Napier grass, Chemosphere, 308 (2022) 136389, doi: 10.1016/j.chemosphere.2022.136389.
[14] X. He, T. Zhang, Q. Xue, Y. Zhou, H. Wang, N.S. Bolan, R. Jiang, D.C.W. Tsang, Enhanced adsorption of Cu(II) and Zn(II) from aqueous solution by polyethyleneimine modified straw hydrochar, Sci. Total Environ., 778 (2021) 146116, doi: 10.1016/j.scitotenv.2021.146116.
[15] F. Dhaouadi, L. Sellaoui, L.E. Hernández-Hernández, A. Bonilla-Petriciolet, D.I. Mendoza-Castillo, H.E. Reynel-Ávila, H.A. González-Ponce, S. Taamalli, F. Louis, A.B. Lamine, Preparation of an avocado seed hydrochar and its application as heavy metal adsorbent: properties and advanced statistical physics modelling, Chem. Eng. J., 419 (2021) 129472, doi: 10.1016/j.cej.2021.129472.
[16] Q. Yin, M. Liu, H. Ren, Biochar produced from the co-pyrolysis of sewage sludge and walnut shell for ammonium and phosphate adsorption from water, J. Environ. Manage., 249 (2019) 109410, doi: 10.1016/j.jenvman.2019.109410.
[17] A. Shaaban, S.-M. Se, N. Merry, M. Mitan, M.F. Dimin, Characterization of biochar derived from rubber wood sawdust through slow pyrolysis on surface porosities and functional groups, Procedia Eng., 68 (2013) 365–371.
[18] S. Rangabhashiyam, K. Vijayaraghavan, Biosorption of Tm(III) by free and polysulfone-immobilized *Turbinaria conoides* biomass, J. Ind. Eng. Chem., 80 (2019) 318–324.
[19] K. Vijayaraghavan, U.M. Joshi, Chicken eggshells remove Pb(II) ions from synthetic wastewater, Environ. Eng. Sci., 30 (2013) 67–73.
[20] M.-Y. Lee, S.-H. Lee, H.-J. Shin, T. Kajiuchi, J.-W. Yang, Characteristics of lead removal by crab shell particles, Process Biochem., 33 (1998) 749–753.
[21] K. Vijayaraghavan, F.D. Raja, Interaction of vermiculite with Pb(II), Cd(II), Cu(II) and Ni(II) ions in single and quaternary mixtures, CLEAN - Soil Air Water, 43 (2015) 1174–1180.
[22] K. Vijayaraghavan, Y.S. Yun, Bacterial biosorbents and biosorption, Biotechnol. Adv., 26 (2008) 266–291.
[23] R. Senthilkumar, K. Saravanakumar, D.M.R. Prasad, B.S.N. Prasad, F. Shaik, Effective batch and column remediation of zinc(II) from synthetic and electroplating effluents using biochar from brown alga, Int. J. Environ. Sci. Technol., 19 (2022) 10317–10324.
[24] G. Limousin, J.-P. Gaudet, L. Charlet, S. Szenknect, V. Barthès, M. Krimissa, Sorption isotherms: a review on physical bases, modeling and measurement, Appl. Geochem., 22 (2007) 249–275.
[25] I. Langmuir, The constitution and fundamental properties of solids and liquids, J. Am. Chem. Soc., 38 (1916) 2221–2295.
[26] H.M.F. Freundlich, About the adsorption in solution, Zeitschrift für Physikalische Chemie, 57 (1906) 385–471.
[27] O. Redlich, D.L. Peterson, A useful adsorption isotherm, J. Phys. Chem., 63 (1959) 1024–1026.
[28] Y.S. Ho, G. McKay, Sorption of dye from aqueous solution by peat, Chem. Eng. J., 70 (1998) 115–124.
[29] K. Saravanakumar, B.S. Naveen Prasad, R. Senthilkumar, D.M.R. Prasad, D. Venkatesan, Single and competitive sorption potential of date seed-derived biochar during removal of lead(II) and cadmium(II) ions, Environ. Prog. Sustainable Energy, 40 (2021) e13690, doi: 10.1002/ep.13690.
[30] K. Saravanakumar, R. Senthilkumar, D.M.R. Prasad, B.S. Naveen Prasad, S. Manickam, V. Gajendiran, Batch and column arsenate sorption using *Turbinaria ornata* seaweed derived biochar: experimental studies and mathematical modelling, ChemistrySelect, 5 (2020) 3661–3668.
[31] F. Cherono, N. Mburu, B. Kakoi, Adsorption of lead, copper and zinc in a multi-metal aqueous solution by waste rubber tires for the design of single batch adsorber, Heliyon, 7 (2021) e08254, doi: 10.1016/j.heliyon.2021.e08254.
[32] H. Chen, W. Li, J. Wang, H. Xu, Y. Liu, Z. Zhang, Y. Li, Y. Zhang, Adsorption of cadmium and lead ions by phosphoric acid-modified biochar generated from chicken feather: selective adsorption and influence of dissolved organic matter, Bioresour. Technol., 292 (2019) 121948, doi: 10.1016/j.biortech.2019.121948.
[33] V.O. Njoku, A.A. Ayuk, E.E. Ejike, E.E. Oguzie, C.E. Duru, O.S. Bello, Cocoa pod husk as a low cost biosorbent for the removal of Pb(II) and Cu(II) from aqueous solutions, Aust. J. Basic Appl. Sci., 5 (2011) 101–110.
[34] A.D. Papandreou, C.J. Stournaras, D. Panias, I. Paspaliaris, Adsorption of Pb(II), Zn(II) and Cr(III) on coal fly ash porous pellets, Miner. Eng., 24 (2011) 1495–1501.
[35] S. Tunali, T. Akar, A.S. Ozcan, I. Kiran, A. Ozcan, Equilibrium and kinetics of biosorption of lead(II) from aqueous solutions by *Cephalosporium aphidicola*, Sep. Purif. Technol., 47 (2006) 105–112.
[36] N.S. Ehishan, N. Sapawe, Performance studies removal of chromium (Cr^{6+}) and lead (Pb^{2+}) by oil palm frond (OPF) adsorbent in aqueous solution, Mater. Today:. Proc., 5 (2018) 21897–21904.